Metal-Dispersed Xerogel-Based Composite Films for the Development of Interference Free Oxidase-Based Biosensors

Beatriz Prieto-Simón,† Gerasimos S. Armatas, Philippos J. Pomonis, Christos G. Nanos, and Mamas I. Prodromidis*

Department of Chemistry, University of Ioannina, 45 110 Ioannina, Greece

Received November 3, 2003. Revised Manuscript Received January 20, 2004

We report for the first time the synthesis of metal-modified 3-aminopropyltrimethoxysilanes (APTMS) and their application for the electrochemical monitoring of hydrogen peroxide. Copper-, iron-, zinc-, and cerium-modified APTMS were mixed with tetraethoxysilane (TEOS) and the finally produced xerogels were characterized with scanning electron microscopy, energy dispersive spectrometry, nitrogen porosimetry, and thermal gravimetry. The potential of these materials as catalytic surfaces for the electrochemical monitoring of hydrogen peroxide was investigated by performing cyclic voltammetry and amperometric measurements of metal−APTMS/TEOS modified-platinum electrodes. Results show a significant increase in the sensitivity of the resulting probes compared with the sensitivity of those modified by APTMS/TEOS. However, their applicability and stability were not satisfactory due to the lack of homogeneity, low adhesion onto the electrode surface, and cracking effects during aging. The aforementioned problems were totally eliminated, and the sensitivity of the electrodes was impressively increased, when the metal-modified xerogels were applied over the platinum electrodes as a mixture in a poly(ethylene glycol)−cellulose acetate composite solution (PEG/CA). Apparent diffusion coefficients for different concentrations of PEG were determined with chronocoulometry. Resistance and wettability of the composite films were evaluated with impedance spectroscopy. Metal−APTMS/TEOS−PEG/CA composite films were also successfully tested in the construction of interference-free biosensors for glucose and hydrogen peroxide by immobilizing glucose oxidase and horseradish peroxidase, respectively, into an ethanol-free TEOS sol−gel layer developed over the composite films.

Introduction

Sol−gel based biosensors have attracted enormous scientific attention, and a plethora of articles dealing with the immobilization of biomolecules into sol−gel matrixes have been published[1−5] and extensively reviewed.[6−7] The majority of the published work on this subject refers to the physical entrapment of the biomolecules into sol−gel silica matrixes.[8−10] In addition, gels based on vanadium pentaoxide,[4] titanium isopropoxide,[11] or organically modified siloxanes that provide direct covalent binding or encapsulation of the proteins by additional cross-linking through bifunctional agents have also been published.[12−13]

Despite the volume of the published work, inherent drawbacks in the development of such gels as immobilizing agents still exist. These include cracking of the films and swelling of the hydrogel, as well as high concentration of ethanol in the resulted sol. To overcome the aforementioned drawbacks, incorporation of a grafting copolymer of poly(vinyl alcohol) with 4-vinylpyridine into the silica sol was found to prevent the cracking of conventional sol−gel-derived glasses and eliminate the swelling of the hydrogel.[14] In addition, an aqueous route for synthesis of silica monoliths with encapsulated

* Corresponding author. Fax: ++30-26510-98796. E-mail: mprodrom@cc.uoi.gr.

† On leave from Department of Chemistry, Universitat Autònoma de Barcelona, E-08193, Spain.

(1) Braun, S.; Rappoport, S.; Zusman, R.; Avnir, D.; Ottolenghi, M. *Mater. Lett.* **1990**, *10*, 1−5.

(2) Ellerby, L. M.; Nishida, C. R.; Nishida, F.; Yamanaka, S. A.; Dunn, B.; Valentine, J. S.; Zink, J. I. *Science* **1992**, *255*, 1113−1115.

(3) Audebert, P.; Demaille, C.; Sanchez, C. *Chem. Mater.* **1993**, *5*, 911−913.

(4) Glezer, V.; Lev, O. *J. Am. Chem. Soc.* **1993**, *115*, 2533−2534.

(5) Gelman, F.; Blum, J.; Avnir, D. *J. Am. Chem. Soc.* **2002**, *124*, 14460−14463. Smith, K.; Silvernail, N. J.; Rodgers, K. R.; Elgren, T. E.; Castro, M.; Parker, R. M. *J. Am. Chem. Soc.* **2002**, *124*, 4247−4252. Gill, I.; Pastor, E.; Ballesteros, A. *J. Am. Chem. Soc.* **1999**, *41*, 9487−9496. Dave, B. C.; Dunn, B.; Valentine, J. S.; Zink, J. I. *Anal. Chem.* **1994**, *66*, 1120−1128A.

(6) Gill, I. *Chem. Mater.* **2001**, *13*, 3404−3421.; Dong, S.; Chen, X. *Rev. Mol. Biotechnol.* **2002**, *82*, 303−323.

(7) Jin, W.; Brennan, J. D. *Anal. Chim. Acta* **2002**, *461*, 1−36.

(8) Wang, J.; Pamidi, P. V. A.; Park, D. S. *Anal. Chem.* **1996**, *68*, 2705−2708.

(9) Cho, E. J.; Tao, Z.; Tehan, E. C.; Bright, F. V. *Anal. Chem.* **2002**, *74*, 6177−6184.

(10) Kumar, A.; Malhotra, R.; Malhotra, B. D.; Grover, S. K. *Anal. Chim. Acta* **2000**, *414*, 43−50.

(11) Cosnier, S.; Senillou, A.; Gratzel, M.; Comte, P.; Vlachopoulos, N.; Renault, N.-J.; Martelet, C. *J. Electroanal. Chem.* **1999**, *469*, 176−181.

(12) Gaspers, P. B.; Gast, A. P.; Robertson, C. R. *J. Colloid Interface Sci.* **1995**, *172*, 518−529.

(13) Advir, D. *Acc. Chem. Res.* **1995**, *28*, 328−334.

(14) Wang, B.; Zhang, J.; Dong, S. *Biosens. Bioelectron.* **2000**, *15*, 397−402.

10.1021/cm035110u CCC: $27.50
Published on Web 02/27/2004

biological entities by using sodium silicate as a precursor,[15] and removal of the ethanol through the application of rotavapor methods[16] have been reported.

Although still in its infancy, the work that has been done regarding the potential of sol−gels as host matrixes of biomolecules will play a major role in future electrochemical biosensing technology. Nevertheless, a considerable amount of fundamental research remains to be done, especially for the development of efficient catalytic materials for the oxidation of hydrogen peroxide and NADH, the two major products of biosensor devices. This is because problems associated with the electrochemical detection of such molecules, namely highly applied overpotentials and fouling of the electrodes surfaces, do not allow the majority of the biosensor-based analytical devices to pass from the academic concept to commercial applications. In addressing such problems, the incorporation of mediators or noble metals in sol−gel networks has been reported.[17−27] We propose here some novel iron-, copper-, cerium-, and zinc-modified xerogels and demonstrate their ability to serve as catalysts for the electrochemical oxidation of hydrogen peroxide. Moreover, composite films of the xerogels, with cellulose acetate serving as an emulsion and a diffusion-controlled agent, and with polyethelene glycol serving as a xerogel-dispersion, wettability-induced, and cracking-preventing agent are also introduced as potential materials for the construction of sensitive and interference-free oxidase-based amperometric biosensors. Their performance as glucose or hydrogen peroxide biosensors is also demonstrated.

Experimental Section

Chemicals. Glucose oxidase type X-S (GOx, EC 1.1.3.4, from *Aspergillus niger*) and peroxidase type VI-A (EC 1.11.1.7, from horseradish) were supplied from Sigma (St. Louis, MO). 3-Aminopropyltrimethoxysilane (APTMS) and tetraethoxysilane (TEOS) were obtained from Merck (Darmstadt, Germany) and used without further purification. Ascorbic acid, hydrogen peroxide (30% w/w), cellulose acetate (CA, 40% acetyl), poly(ethylene glycol) 650 (PEG), and β-D(+)-glucose were also purchased from Sigma. $Ce(NO_3)_3{\cdot}xH_2O$, $Cu(SO_4){\cdot}5H_2O$, $FeCl_3{\cdot}6H_2O$, and $ZnCl_2{\cdot}xH_2O$ of analytical grade were obtained from Riedel-de Haen (Seelze, Germany). All other chemicals were of analytical grade from Merck and Sigma. Double distilled water (DDW) was used throughout. A stock solution of approximately 0.2 M H_2O_2 was prepared by appropriate dilution of the concentrated solution in DDW, stored at +4 °C, and standardized weekly with the $KMnO_4$ titrimetric method. A stock solution of glucose (0.2 M in DDW) was prepared 24 h before use.

Electrochemical Studies. All electrochemical experiments were conducted with a computer-controlled potentiostat, AUTOLAB (EcoChemie, The Netherlands), in a 15-mL voltammetry cell (VC2, BAS, U.S.) using a platinum electrode (1.6 mm i.d., BAS) as the working electrode, a Ag/AgCl/3M KCl (BAS) as a reference electrode, and a Pt wire as an auxiliary electrode (BAS). Prior to use, working electrodes were polished with Al_2O_3 over a wool cloth, sonicated in DDW for 3 min, and washed thoroughly with DDW and ethanol.

Preparation of the Metal-Modified Xerogels. A homogeneous solution was prepared by mixing a metallic precursor M ($M = Ce^{4+}$, Cu^{2+}, Fe^{3+}, Zn^{2+}) and 0.5 mL of APTMS with molar ratio M/APTMS = 1 in a glass tube with 25 mL of methanol. The mixture was kept at room temperature for 1 h under continuous stirring. Then 0.65 mL of TEOS (TEOS/APTMS molar ratio = 1), 1 mL of deionized water (H_2O/TEOS molar ratio = 10), and 1 mL of aqueous ammonia (25% w/w) as catalyst, were added. After 2 h at room temperature and under stirring, the resulting solid was recovered by filtration (Whatman #40), washed with ethanol and distilled water, and dried at 110 °C for 12 h.

Nitrogen Adsorption−Desorption Measurements. A Fisons Sorptomatic 1900 instrument was used to carry out the pore size distribution measurements. The characterization included the determination of nitrogen adsorption−desorption isotherms at 77 K. Prior to each adsorption−desorption measurement, the samples were degassed at 50 °C in a vacuum of 5×10^{-2} mbar for 12 h. The desorption branch of the isotherms was used for calculation of the pore size distribution (PSD). PSD and the specific surface area of the sample were calculated by applying the BET equation using the linear part ($0.05 < P/P_o < 0.30$) of the adsorption isotherm.

Thermogravimetry. Thermogravimetry and differential thermal analysis (TG−DTA) were carried out with a Shimadzu DTG-60 instrument with a heating rate of 10 °C min^{-1} under a flow of 50 cm^3 min^{-1} dry air.

Scanning Electron Microscopy−Energy Dispersive Spectrometry (SEM−EDS) Analysis. SEM images were taken with a JEOL JSM-5600 scanning electron microscope. EDS analysis was performed using an ISIS-300 microanalysis system by Oxford Instruments. Samples were coated with a 25-nm-thick film of Au/Pd using a Polaron SC7620 sputter-coater by Thermo VG Scientific.

Assembly of the Biosensors. *Proposed Biosensors Based on Two-Membrane Architecture. Inner Membrane.* A mixture of 10 mg of metal-modified xerogels, 0.8 mL of 2% solution of cellulose acetate, and 0.2 mL of PEG was prepared and left to homogenize under stirring overnight. An aliquot of 10 μL of the final mixture was applied over the electrode surface and allowed to air-dry. *Outer Membrane.* GOx- or peroxidase-modified ethanol-free sol−gel films of tetraethoxysilane were prepared according to a previously described method.[15] An aliquot of 10 μL of the final mixture corresponding to 100 U GOx or peroxidase was applied over the metal-modified xerogel/CA/PEG composite film and allowed to air-dry. The thickness of the resulting membranes was measured with a digital thickness meter and was found to be 15 ± 2 μm.

Analytical Procedure. A $(10.0 - x)$-mL aliquot of 0.25 M phosphate buffer (pH 6.5 or 7.0) was introduced in the reaction cell and stirred at a moderate speed with a magnetic stirrer. When a stable current value was reached appropriate amounts (x mL) of hydrogen peroxide or glucose solutions were added, and current changes due to the hydrogen peroxide reduction at −0.2 V or oxidation at +0.65 V versus Ag/AgCl/3M KCl were recorded. The steady-state current response (within 20 s) was taken as a measure of the analyte concentration.

Results and Discussion

Optimization of the Synthetic Route. Initial experiments for the preparation of metal-modified sol−gels were carried out using iron (III) chloride and

(15) Ferrer, M. L.; del Monte, F.; Levy, D. *Chem. Mater.* **2002**, *14*, 3619−3621.
(16) Bhatia, R. B.; Brinker, C. J. *Chem. Mater.* **2002**, *12*, 2434−2441.
(17) Khoo, S. B.; Chen, F. *Anal. Chem.* **2002**, *74*, 5734−5741.
(18) Zhang, L.; Lin, B.; Wang, Z.; Cheng, G.; Dong, S. *Anal. Chim. Acta* **1999**, *388*, 71−78.
(19) Sampath, S.; Lev, O. *Electroanalysis* **1996**, *8*, 1112−1116.
(20) Wang, J.; Pamidi, P. V. A. *Anal. Chem.* **1997**, *69*, 4490−4494.
(21) Gill, I.; Ballesteros, A. *J. Am. Chem. Soc.* **1998**, *120*, 8587−8598.
(22) Niu, J.; Lee, J. Y. *Sens. Actuators B* **2000**, *62*, 190−198.
(23) Li, J.; Chia, L. S.; Goh, N. K.; Tan, S. N. *Anal. Chim. Acta* **1998**, *362*, 203−211.
(24) Chen, X.; Wang, B.; Dong, S. *Electroanalysis* **2001**, *13*, 1149−1152.
(25) Wang, B.; Dong, S. *Talanta* **2000**, *51*, 565−572.
(26) Chen, X.; Zhang, J. Z.; Wang, B. Q.; Cheng, G. J.; Dong, S. J. *Anal. Chim. Acta* **2001**, *434*, 255−260.
(27) Lu, Z.-L.; Lindner, E.; Mayer, H. A. *Chem Rev.* **2002**, *102*, 3543−3578 and references therein.

Scheme 1. Schematic Reaction Pathway for Preparation of the Metal-APTMS/TEOS Sol−Gel.

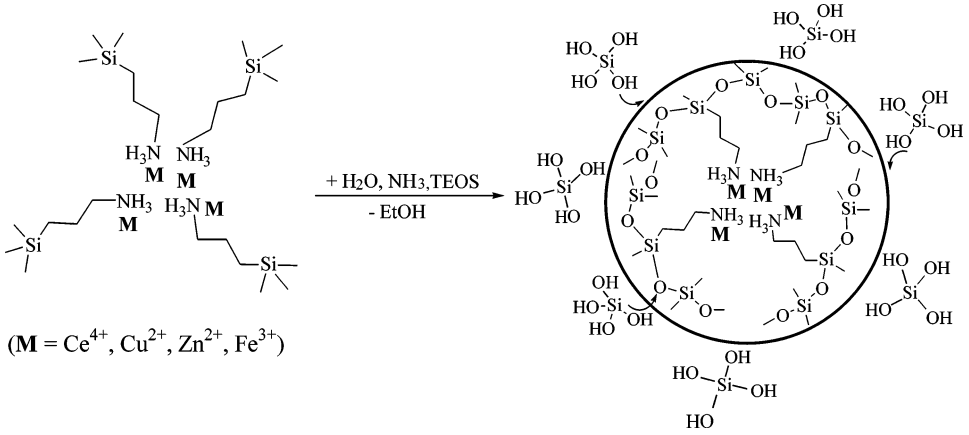

Table 1. Physical and (Electro)Chemical Properties of the Metal-Modified Sol−Gel Composite Films

electrode assembly	mechanical strength/solubility	R. E. (%)[a]	interference effect of 5 mM ascorbic acid/uric acid /dopamine[d]	anodic catalytic current[e] (μA)/ voltage[f] (V)	cathodic catalytic current[e] (μA)/ voltage[f] (V)
Pt/Fe−SG (1:2.5)[b]	poor/high	175			
Pt/Cu−SG (1:2.5)[b]	poor/high	176			
Pt/Zn−SG (1:2.5)[b]	very poor/quite high	180			
Pt/Ce−SG (1:2.5)[b]	very poor/quite high	195			
Pt/Fe−SG/CA (1:0.5)[c]	good/nonsoluble	115		0.9/0.75	42/0.01
Pt/Fe−SG/CA (1:1)[c]	very good/nonsoluble	103	2/1/4	1.9/0.67	88/0.03
Pt/Fe−SG/CA (1:2)[c]	very good/nonsoluble	101		4.9/0.75	27/0.01
Pt/Cu−SG/CA (1:1)[c]	very good/nonsoluble	104		5.4/0.64	48/−0.09
Pt/Zn−SG/CA (1:1)[c]	very good/nonsoluble	102	3/1/4	3.4/0.51	85/−0.07
Pt/Ce−SG/CA (1:1)[c]	very good/nonsoluble	102	3/0/2	3.8/0.67	22/−0.07

[a] Relative efficiency (relative response for mixed solutions of 5 mM ascorbic acid and 2.5 mM hydrogen peroxide, compared to the response shown with pure solution of 2.5 mM hydrogen peroxide taken as 100%). [b] SG: water dilution ratio. [c] SG: CA dilution ratio. [d] Relative response of the sensors in the presence of 5 mM pure solutions of ascorbic acid/uric acid/dopamine, compared to the response shown with pure solution of 2.5 mM hydrogen peroxide taken as 100%. [e] Peak height corrected with the baseline. [f] Peak potential and peak currents extracted from the CV-grams.

APTMS. Covalent bonding between the metal and the nitrogen of the silane (Fe−APTMS) was attempted in methanol and THF. In each case, both acidic (HCl) and basic (NH_4OH) catalysts were used. New materials were evaluated, setting as criteria the solubility and the mechanical stability of the resulting films onto the platinum electrodes, as well as the sensitivity (cathodic current, corrected by the baseline attributed to the corresponding non-metal-modified material) of the latter, as hydrogen peroxide probes by performing cyclic voltammetry (CV) experiments. To increase the hydrophobicity of the metal-modified sol−gels, condensation of the Fe−APTMS silane was carried out in the presence of different amounts of TEOS (0.5:1, 1:1, and 2:1 molar ratios with respect to APTMS) (Scheme 1). Best results in terms of film stability were obtained in cases of 1:1 and 2:1 silane mixtures in methanol and basic catalyst. Further experiments were carried out with the equal molar silane mixture, as the 2:1 silane mixture provides less metal sites in the silica matrix.

Development of the Composite Films. Aiming to develop a multifunctional composite film able to ensure high-performance sensors, that is, protection from various interferants and electrode fouling, as well as the establishment of a mass-controlled transport mechanism (the latter ensures wider dynamic range), we investigated the behavior of different mixtures of the optimum iron-modified sol−gel with water (1:0.5−1:10 v/v) (data not shown) and 4% cellulose acetate (1:0.5−1:2 v/v) solution. Following a single parameter optimization study, a mixture produced from the dilution of the gel with water (1:2.5 v/v) and then mixed with an equal volume of 4% cellulose acetate was found to be the optimum (see Table 1). A cumulative presentation of some of the mechanical and electrochemical characteristics of the tested electrode assemblies is given in Table 1.

Following the optimum conditions in both the synthetic route and the film preparation, we also proceeded with construction of zinc(II)-, copper(II)-, and cerium(IV)-modified sol−gel (SG) cellulose acetate (CA) composite film electrodes.

The effectiveness of the composite film in behaving as a molecular diffusional barrier with a nominal MW cut-off able to ensure interference-free (bio)sensors was tested by using ascorbic acid (MW 176.2 Da), uric acid (MW 168.1 Da), and a neutral compound, dopamine (MW 151.2), as model compounds. Cellulose acetate films have been well documented in the literature as effective diffusional barriers.[28] The overall effect of the sol−gel matrix was tested with CV experiments and a comparative study is given in Table 1. Because of the nature of the immobilized metal ions (high concentration, entrapment in the silica matrix, and interactions of adjacent silicon-bridged atoms),[17] blank CVs of the tested materials (data not shown), showed very weak peaks that are not able to provide useful information.

(28) Cass, A. E. G., Ed. *Biosensors: A Practical Approach*; Oxford University Press: Oxford, 1990; Ch. 1.

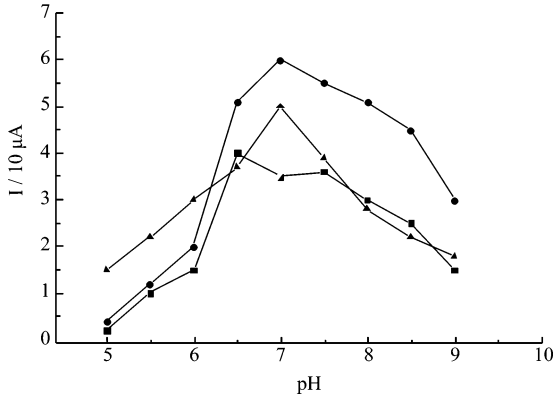

Figure 1. pH profile of (●) zinc-, (■) iron-, and (▲) cerium-modified XG/CA/PEG composite films; applied voltage 0.65 V; 5 mM H_2O_2; 50 mM phosphate in 50 mM KCl.

The pH of the working buffer was investigated by performing steady-state amperometric measurements in a 50-mM phosphate buffering system covering the pH range 5−9. Comparative results are shown in Figure 1.

Scanning Electron Microscopy. Figure 2 shows the SEM images of samples dried at 110 °C. The sample without metal is composed of relatively big dense particles (data not shown). Samples of copper- and iron-modified xerogels are composed of both loose and dense aggregations of particles. The loose aggregations form circles, and the enlargement (data not shown) of their circular section shows that these particles are irregularly condensed and adopt a heterogeneous structure composed of masses of various sizes. However, the greater part of the gel is in the form of dense aggregations and is also composed of small particles. Such structure inhomogeneities of silica result mainly from the phase separation of unhydrolyzed TEOS. In present work, though the amount of water used was large enough (H_2O/TEOS = 10), it seems that the hydrolysis was not completed or that it took place very slowly compared with the hydrolysis and condensation of the APTMS. On the other hand, the gels of zinc- and cerium-modified xerogels are composed of dense aggregation of small spherical particles of about 500 and 300 nm, respectively, packed closely as shown in Figure 2.

The materials were also studied with EDS analysis to obtain a rough estimate of the amount of metal located on their external surface. As can be seen from the images illustrated in Figure 3 there is an excellent dispersion of the metals over the surface of the particles, except in the case of copper, where separated $Cu(OH)_xO_y$ particles over the silica matrix were observed. The dispersion of the metals should be attributed to the amino groups of the APTMS, which actually act as metal binders thus preventing the formation of metal conglomerates. The formation of copper conglomerates can be attributed to the effect of the NH_3 catalyst on the Si−Cu bonds and the formation of the soluble $[Cu(NH_3)]^{2+}$ complex that is further weakly absorbed or entrapped in the silica matrix during the polycondensation process of the sol.

The ratio of the surface concentration of the metal to the total concentration was also calculated with EDS analysis (average of 10 points) and post chemical analysis of the metals in the various xerogels with polarography (copper and zinc) and iodometric back-titration (cerium and iron) prior to their dilution in 4 N HCl at 40 °C for 2h.[29] From the values in Table 2 we can observe that in cases of iron-, zinc-, and cerium-modified xerogels almost one-third of the metal lies on the surface while the rest of the metal is found (probably encapsulated) in the interior of the silica matrix. This does not occur for copper-modified xerogel where almost 80% of the total concentration is located on the outermost layer of the particles.

N_2 Adsorption−Desorption Isotherms. Specific surface areas S_P ($m^2\ g^{-1}$) and the specific pore volume V_P ($cm^3\ g^{-1}$) are given in Table 2. The unmodified material as well as the materials modified with cerium, zinc, and iron give rise to isotherms characteristic of solids without internal porosity, and possessing low

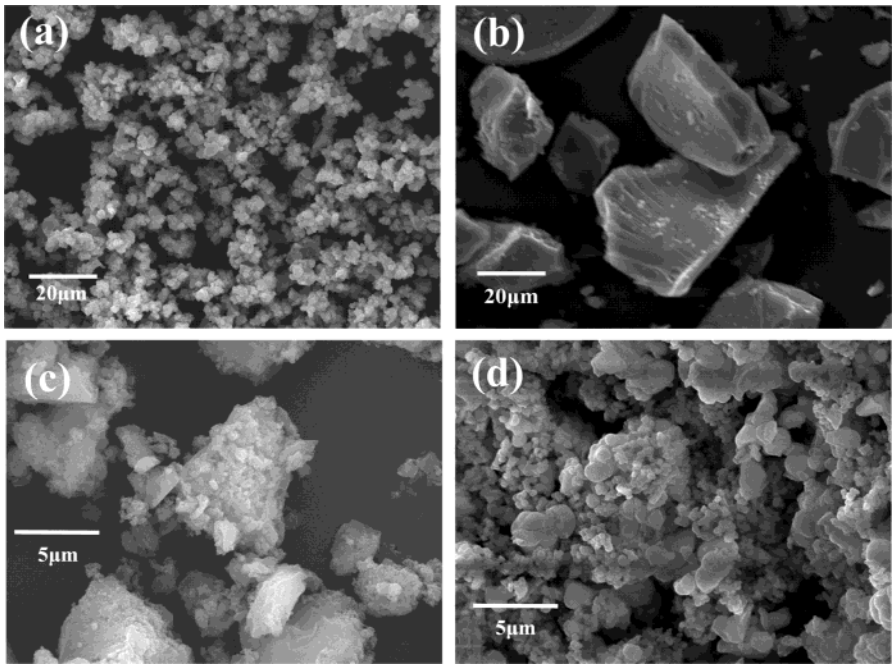

Figure 2. SEM images of (a) zinc-, (b) iron-, (c) copper-, and (d) cerium-modified xerogels.

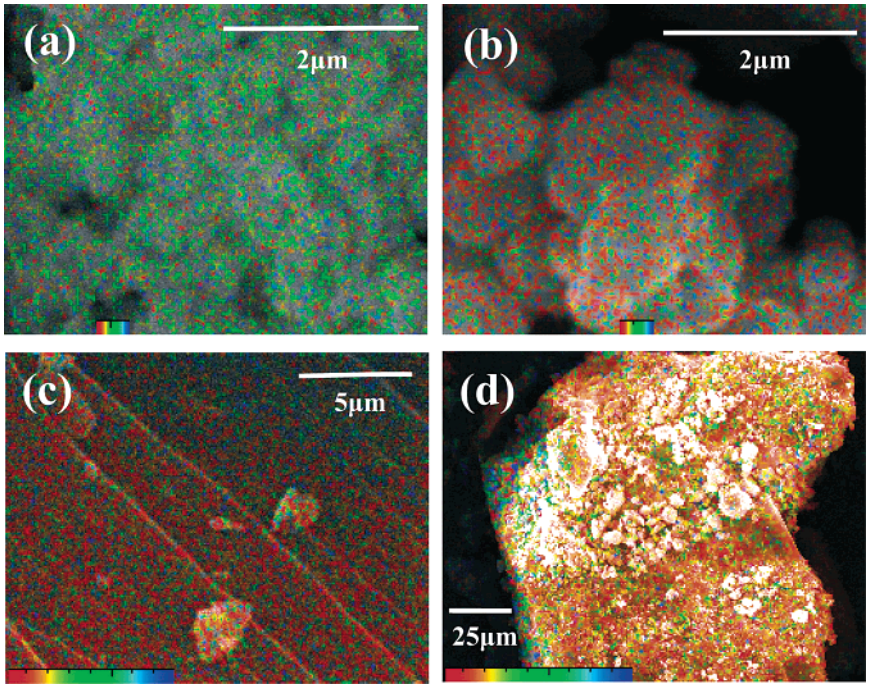

Figure 3. EDS analysis of the (a) cerium-, (b) zinc-, (c) iron-, and (d) copper-modified xerogels. The characteristic X-ray peaks are: Si, 1.74 keV; Zn, 8.63/1.01 keV; Ce, 4.84/0.88 keV; Cu, 8.04/0.93 keV; Fe, 6.40/0.70 keV. Color scales and corresponding energy ranges: (a) 4.40−6.00 keV; (b) 8.40−10.00 keV; (c) 0.20−8.00 keV; (d) 0.20−9.00 keV.

Table 2. Surface and Total Concentrations of Metals, Specific Surface Area (S_p), Specific Pore Volume (V_p), Percentage Weight Loss, and the Corresponding mmol of $H_3N-(CH_2)_3Si(O^-)_3$ Per Gram Burned during the TG−DTA Experiments in Various Metal-Modified Xerogels

sample	surface conc. (%)[a,b]	total conc. (%)[a,c]	surface/total concn ratio (%)	S_p ($m^2\ g^{-1}$)	V_p ($cm^3\ g^{-1}$)	weight loss (%)	(mmol g^{-1})[d]
nonmetal XG				<10	0.01	25.74	1.92
Cu-modified XG	8	10	80	103	0.12	21.71	1.62
Fe-modified XG	13	33	40	11	0.02	21.35	1.59
Ce-modified XG	7	20	35	10	0.01	26.83	2.00
Zn-modified XG	10	37	27	18	0.35	24.68	1.84

[a] The standard deviation of the mean ranges from 0.2 to 1%. [b] EDS. [c] Post chemical analysis. [d] The immobilized organic groups were calculated as hydrolyzed residual $H_3N-(CH_2)_3Si(O^-)_3$.

surface area ($S_p \approx 10-18\ m^2g^{-1}$), which is due to the external surface of particles. The only material with a relatively high specific surface area (103 m^2g^{-1}) and internal porosity is the one based on copper (data not shown). It is of interest that the latter material has the highest % ratio of surface/total metal concentration (Table 2) and its surface contains $Cu(OH)_xO_y$ conglomerates (see SEM image in Figure 2 and EDS data in Figure 3). We can therefore assume that the calculated relatively high specific area and observed internal porosity of this material are due to the $Cu(OH)_xO_y$ particles and not to the $Me-SiO_2$ matrix containing the metal in good dispersion over the whole of its mass. The specific pore volume V_p of the metal-modified xerogels was found to be low (Table 2), and only in the zinc-modified xerogel was the specific pore volume found to be particularly high ($V_p \approx 0.35\ cm^3g^{-1}$, see Table 2). This is attributed to the particular texture of this material (see SEM image in Figure 2), as well as to the big interparticle volume of it, which is constituted of good stacked uniform particles.

Thermogravimetry. The results of the TG−DTA studies in the range of 150−550 °C indicate the weight loss corresponding to the amount of anchored organic groups burned during heating. The calculated % weight loss and the mol of residual $H_3N-(CH_2)_3Si(O^-)_3$ per gram of solids are given in Table 2. We observe that the % weight loss is almost steady around 21−26% and that it corresponds to 1.6−2.0 mmol g^{-1} of $H_3N-(CH_2)_3Si(O^-)_3$. This percentage is very close to the theoretically expected weight loss, if we consider that one $H_3N-(CH_2)_3-$group is bonded with two SiO_2 entities. Any deviations from the theoretical values could be attributed to the water content.

Metal-Modified Xerogels−Polyethylenglycol-Modified Cellulose Composite Films. Corresponding xerogels (XG) were found to be well homogenized in the cellulose acetate solution, giving thus an almost clear viscous solution. Films produced in this manner and the resulted electrodes were tested as electrochemical probes for the determination of hydrogen peroxide. All the tested metal-bearing films gave no electrochemical response. This behavior could be attributed to the lack of conductivity of the resulting films, the extremely low diffusion of the target analyte through the films, the

(29) Polarograms were taken in a 50-mL cell in 0.2 M HCl, 0.01% gelatin, and one drop of *n*-octanol electrolyte mixture at 25 °C by using a Tacussel (recorder EPL-1B, polarographic module TIPOL) voltammetric analyzer. A three-electrode system consisted of a dropping mercury working electrode, a saturated calomel reference electrode, and a platinum auxiliary electrode was used. The scan rate was 150 mVs^{-1}. Before the samples were measured, they were deaerated with nitrogen.

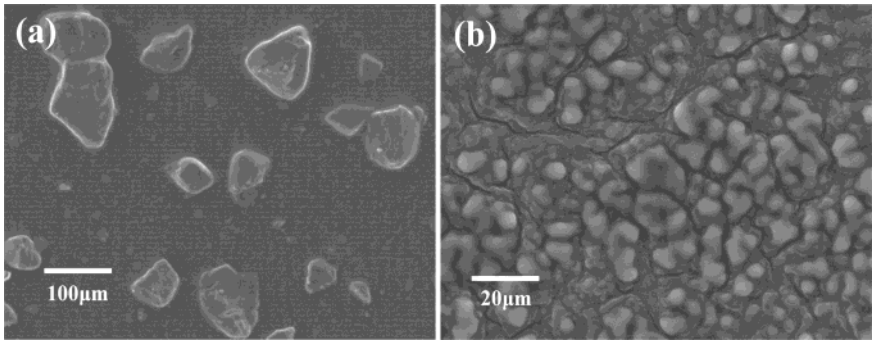

Figure 4. SEM images of (a) iron-modified XG/CA and (b) iron-modified XG/CA/PEG 20% composite films.

Table 3. Diffusion Coefficients (D_{app})

	diffusion coefficients, $cm^2\ s^{-1}$		
xerogel/analyte [a]	Pt/XG/CA	Pt/XG/CA/20% PEG	Pt/XG/CA/30% PEG
Ce-xerogel/H_2O_2	1.26×10^{-9}	6.88×10^{-6}	1.50×10^{-6}
Ce-xerogel/ascorbate	7.98×10^{-10}	2.71×10^{-6}	1.08×10^{-6}
nonmodified xerogel/H_2O_2	2.63×10^{-9}	1.07×10^{-6}	7.47×10^{-7}

[a] Concentrations of 5 mM of the tested compounds in a 0.25 M phosphate buffer (pH 6.5) in 0.5 M KCl were used.

limited wettability of the films, or, finally, to a combination of these reasons. A detailed experimental study of each of the above-mentioned reasons is given below. Addition of PEG into the metal-modified XG/CA mixture gave films of sufficient effectiveness to the electrosensing of hydrogen peroxide. Investigating the exact mechanism of the action of PEG, various diagnostic experiments were performed to distinguish between the conductivity and the electrocatalytic ability of each membrane. Confusion is often noted in the literature because these terms are treated or meant as the same. This is because the overall behavior of a sensor, that is, a measurable catalytic current, is the result of the above-mentioned parameters. The effect of PEG on the overall response of the composite films was studied within the concentration range 0−40% v/v with respect to the volume of polymeric solution. The magnitude of the catalytic current raised after the addition of 2.5 mM H_2O_2 was taken as a criterion for the selection of the optimum concentration. Best results were obtained at a concentration of 20% v/v (data not shown). Higher concentrations result in electrodes with lower electrocatalytic activity, probably due to the lowering of the concentration of the metal-active xerogels in the composite films.

Apart from the case of a high electronic-conductivity film, in which the polymer−solution interface is the "electrode" surface and intrinsic electroactivity takes place at the film−solution interface, all other kinds of conductive films (redox, ion-exchange, or those based on a charge transport mechanism) are strictly dependent on the partition and the diffusion of the target analyte into and through the film. Another important parameter that affects the overall electrocatalytic behavior of the film is the hydrophobic/hydrophilic nature, that is the wettability, which expresses the ability of the analyte and solvent to approach or penetrate the film and facilitating thus adequate ionic mobility and lower film ohmic resistance. Finally, the large quantity of the metal redox sites in the film enhances the electrocatalytic rate as compared to monolayers, but this advantage depends on the ability of the substrate to penetrate the film. Regarding the latter condition, factors such as the charge of the analyte, its steric bulk, and the thickness of the film, which are also relevant factors, were not taken into account, as they are considered constant in all cases. The even distribution of the xerogel particles spread around the film is also an important parameter, as it ensures a high number of collisions among the molecules of the analyte and the catalytic sites. As can be seen from the SEM images in Figure 4, the presence of PEG in the composite films effectively contributed to the even distribution of the xerogel within the composite films.

Diffusion Coefficients. (Apparent) diffusion coefficients of hydrogen peroxide and ascorbic acid were calculated by double-step chronocoulometry.[30] The potential was stepped from an initial value $E_i = -0.6$ V up to $E_s = +0.3$ V for H_2O_2 and $E_s = +0.6$ V for ascorbic acid and finally stepped back to E_i. As can be seen from the values illustrated in Table 3, D_{app} increases significantly—almost 3−4 orders of magnitude in the case of the PEG-modified films.

Impedance Spectroscopy and Capacitance Measurements. Conductivity of the various nonmodified and metal-modified xerogels/CA composite films and the effect of PEG on the overall resistance of the films were investigated with EIS. Impedance (real) was measured against potential from −0.2 to 0.6 V at a 50 mM phosphate buffer of pH 7 in 50 mM KCl versus a Ag/AgCl/3M KCl reference electrode. At the potential window +0.1 to +0.3 V (see Figure 5), there is no faradaic reaction, so the film-covered electrodes can be represented by an RC-circuit consisting of the film resistance and double-layer capacitance. Moreover, all the experiments were carried out at a 20 kHz frequency (the voltage amplitude of the sine waveform is 10 mV) to drastically suppress the contribution of the capacitance to the overall impedance and to ensure thus that the recorded impedance is largely attributed to the film resistance. Modification of the film with the various metals resulted in lowering of the apparent resistance

(30) Heineman, W. R. *Curr. Sep.* **1986**, *68*, 2015−2021. Prodromidis, M. I.; Veltsistas, P. G.; Karayannis, M. I. *Anal. Chem.* **2000**, *72*, 3995−4002.

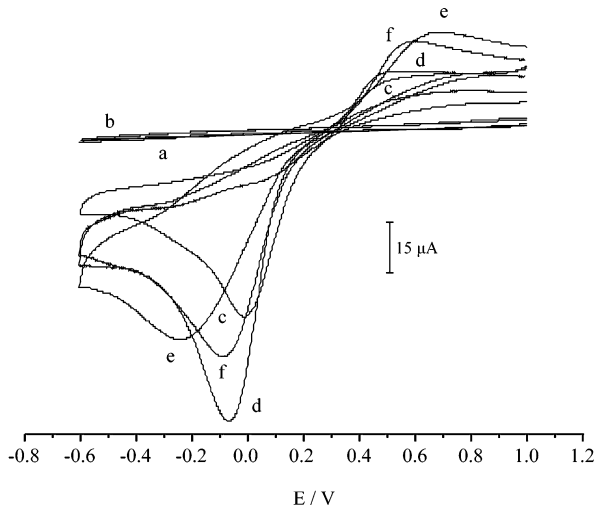

Figure 5. CVs of non-metal-modified XG/CA/PEG composite films at (a) pH 7 and (b) pH 6.5. Scan (c) shows the behavior of the iron-modified SG/CA film at pH 7 and scans (d), (e), and (f) show the behavior of the zinc-, copper-, and cerium-modified XG/CA/PEG composite films at pH 6.5, respectively, over the same potential window: 5 mM H_2O_2; 50 mM phosphate in 50 mM KCl; scan rate 0.1 Vs^{-1}.

Table 4. Evaluation of the Resistance and Wettability of Various Electrode Assemblies

electrode assembly	Z'^a (Ohm)	$Cs^{a,b}$ ($\mu F\ cm^{-2}$)
nonmodified xerogel/CA	4.01×10^3	0.04
Zn-modified xerogel/CA	3.11×10^3	3.3
Fe-modified xerogel/CA	3.56×10^3	1.7
Ce-modified xerogel/CA	1.92×10^3	23.4
nonmodified xerogel/CA/PEG	0.33×10^3	110
Zn-modified xerogel/CA/PEG	0.29×10^3	142
Fe-modified xerogel with/CA/PEG	0.22×10^3	171
Ce-modified xerogel with/CA/PEG	0.31×10^3	115

[a] Values were extracted from the plot $Z' = f(V)$ at the voltage 0.1 V. [b] The total effective electrode area of the platinum electrode was determined by performing double step chronocoulometry of hexacyanoferrate ($D_f = 7.6 \times 10^{-6}\ cm^2\ s^{-1}$, at pH 3).

at a ratio of almost 1:2. Lower resistances were obtained at the PEG-treated films, where the resistance of the films (including the nonmetal modified one) was decreased at a ratio of up to 1:16 (Table 4).

Sampath and Lev[31] have well documented the relation between wettability and hydrophobicity and have shown that capacitance can be used as a semiquantitative measure of the wetted section. In this study, the capacitance of the tested films was measured by registration of the 90° component of the AC current at 80 Hz, according to the Bode plot of the tested assemblies (data not shown), under various DC potentials within the potential window −0.6 to 0.6 V. Results shown in Table 4 are indicative of the great enhancement of the wetted surface area of the PEG-modified composite films. Under optimum conditions, a comparative CV study of all metal-modified xerogel−CA films was obtained as is illustrated in Figure 5.

Application to Standard Solutions of Hydrogen Peroxide. Taking as criteria the sensitivity and the dynamic range of the probes for measuring hydrogen peroxide at +0.65 V, Ce- and Zn-modified SG/CA/PEG films were found to be the most effective. Iron-modified SG/CA/PEG films did not improve the performance of the probe in terms of sensitivity, compared with the results obtained with a CA/PEG-, CA-, and nonmetal modified SG/CA/PEG-modified electrodes. The same study was also carried out in the cathodic region, at −0.2 V. Zn-modified SG/CA/PEG films were found to be the most effective. Cu-modified SG/CA/PEG films did not display any catalytic effect on either the oxidation or the reduction of hydrogen peroxide. This behavior is mainly attributed to the instability of the Cu-modified SG/CA/PEG stock mixture. A chromatic change from blue to dark-green was observed within a few hours after its preparation. The analytical characteristics of the various probes are summarized in Table 5.

Trying to elucidate the obtained results, the following three issues were raised: (i) the ability of some of the surfaces to catalyze both the oxidation and the reduction of hydrogen peroxide, (ii) the nature of the catalytic properties of surfaces modified by zinc, which is a nonredox metal ion, and (iii) the disability of copper-modified surfaces to provide sufficient electrocatalytic activity for the oxidation and/or the reduction of hydrogen peroxide. The ability of some metal-modified surfaces to catalyze both the oxidation and the reduction of hydrogen peroxide has already been proposed.[32−34] For cerium- and iron-modified electrodes presented in this work, the reduction of hydrogen peroxide can be explained according to the following equations, through the formation of free radicals (hydroxyl radical)

$$Me^{n+} + H_2O_2 \rightarrow Me^{(n+1)+} + {}^{\bullet}OH + OH^- \qquad (Me^{n+} = Fe^{2+} \text{ or } Ce^{3+})$$

or, in case of the latter, through electrogenerated Fe(II) by the Fenton reaction

$$Fe^{2+} + H_2O_2 \rightarrow FeO^{2+} + H_2O$$

$$FeO^{2+} + Fe^{2+} + H^+ \rightarrow Fe(OH)^{2+} + Fe^{3+}$$

$$Fe(OH)^{2+} + H^+ \rightarrow Fe^{3+} + H_2O$$

For the oxidation of hydrogen peroxide a mechanism based on the formation of free radicals (perhydroxyl radical)

$$Me^{n+} + H_2O_2 \rightarrow Me^{(n-1)+} + HO_2^{\bullet} + H^+ \qquad (Me^{n+} = Fe^{3+} \text{ or } Ce^{4+})$$

can be assumed. According to the above-mentioned mechanisms, the behavior of the redox-based metal-modified surfaces can be rationally explained.

The electrocatalytic mechanisms described above are valid, mostly, for the metal ions located across the platinum-film interface. These ions can be easily affected by the applied potential, thus changing their oxidation states according to the experimental conditions (0.65 or −0.2 V). On the other hand, metal ions located within the silica matrix or across the film−

(31) Sampath, S.; Lev, O. *Anal. Chem.* **1996**, *68*, 2015−2021.

(32) Somasundrum, M.; Kirtikara, K.; Tanticharoen, M. *Anal. Chim. Acta* **1992**, *259*, 211−218.

(33) Pei, J.; Li, X.-y. *J. Electroanal. Chem.* **1998**, *441*, 245−258.

(34) Shankaran, D. R.; Uehara, N.; Kato, T. *Biosens. Bioelectron.* **2003**, *18*, 721−728.

Table 5. Analytical Characteristics of the Hydrogen Peroxide Chemical Sensors, Glucose Biosensors, and Hydrogen Peroxide Biosensors

electrode assembly	linear range (M)	slope (A/M)	LOD (μM)	r^2	RSD[a] (%)
A. Electrodes for the Determination of H_2O_2					
1. Oxidation of H_2O_2					
Pt/CA	$4 \times 10^{-6} - 3.5 \times 10^{-4}$	0.00712	4	0.9846	
Pt/CA/PEG	$4 \times 10^{-6} - 3.5 \times 10^{-4}$	0.00666	4	0.9997	
Pt/XG/CA/PEG	$8 \times 10^{-6} - 3.5 \times 10^{-4}$	0.00699	6	0.9998	
Pt/XG(Ce)/CA/PEG	$8 \times 10^{-7} - 8 \times 10^{-4}$	0.03753	0.4	0.9999	2.2
Pt/XG(Zn)/CA/PEG	$8 \times 10^{-7} - 8 \times 10^{-4}$	0.01886	0.8	0.9992	2.8
Pt/XG(Fe)/CA/PEG	$4 \times 10^{-6} - 3.5 \times 10^{-4}$	0.00735	4	0.9999	
Pt/XG(Cu)/CA/PEG	$8 \times 10^{-6} - 3.5 \times 10^{-4}$	0.00427	8	0.9985	
2. Reduction of H_2O_2					
Pt/CA	$4 \times 10^{-5} - 3.5 \times 10^{-4}$	−0.00122	25	0.9985	
Pt/CA/PEG	$2 \times 10^{-5} - 3.5 \times 10^{-4}$	−0.00143	15	0.9998	
Pt/XG/CA/PEG	$4 \times 10^{-5} - 3.5 \times 10^{-4}$	−0.00179	30	0.9996	
Pt/XG(Ce)/CA/PEG	$4 \times 10^{-6} - 6 \times 10^{-4}$	−0.00454	2	0.9956	2.6
Pt/XG(Zn)/CA/PEG	$4 \times 10^{-6} - 6 \times 10^{-4}$	−0.00782	1	0.9968	2.6
Pt/XG(Fe)/CA/PEG	$2 \times 10^{-6} - 6 \times 10^{-4}$	−0.00501	2	0.9997	3.1
Pt/XG(Cu)/CA/PEG	$4 \times 10^{-5} - 3.5 \times 10^{-4}$	−0.00157	25	0.9989	
B. Glucose Biosensors (Oxidation of H_2O_2 at +0.65 V)					
Pt/XG(Ce)/CA/PEG/GOx	$5 \times 10^{-6} - 1 \times 10^{-3}$	0.00169	3	0.9993	2.2
Pt/XG(Zn)/CA/PEG/GOx	$4 \times 10^{-6} - 1 \times 10^{-3}$	0.00178	2	0.9994	3.8
Pt/XG(Fe)/CA/PEG/GOx	$8 \times 10^{-6} - 1 \times 10^{-3}$	0.00124	6	0.9996	2.5
C. HRP-Based Biosensors (Reduction of H_2O_2 at −0.2 V)					
Pt/XG(Ce)/CA/PEG/HRP	$8 \times 10^{-6} - 1 \times 10^{-3}$	−0.01089	5	0.9993	2.4
Pt/XG(Zn)/CA/PEG/HRP	$1 \times 10^{-5} - 1 \times 10^{-3}$	−0.00890	8	0.9993	3.9
Pt/XG(Fe)/CA/PEG/HRP	$8 \times 10^{-6} - 1 \times 10^{-3}$	−0.01099	4	0.9993	3.1

[a] Relative standard deviation (0.1 mM H_2O_2, n=5).

solution interface are almost not susceptible to the changes of the applied voltage.

The ability of zinc-modified surfaces to provide sensitive hydrogen peroxide sensors in both the anodic and the cathodic region can be explained by taking into account a more complex mechanism for judging the origin of the measuring signal. It is well-known that various metal oxides act as catalysts for the decomposition of hydrogen peroxide.[35] This heterogeneous catalysis has a nonelectrocatalytic nature and produces, besides H_2O and O_2, various electroactive intermediates, for example ·OH and/or HOO· radicals, that can easily undergo redox reactions when diffusing the silica matrix reach the anodic or cathodic platinum surface.[36] This assumption is in accordance with the results presented in Table 2 (Zn-XG has the biggest specific pore volume and the lowest surface/total concentration ratio). The notable exception among the tested redox metal-modified surfaces was that of Cu-modified SG/CA/PEG films. Besides the instability of the Cu-modified SG/CA/PEG stock mixture mentioned above, copper-based conglomerates that lie on the external surface (not covalently bonded with the silica matrix as in the case of the rest of the tested materials) of the silica matrix are probably leached-out during the preparation of the composite mixture (CA and PEG).

Development of Biosensors. For the development of a glucose biosensor, metal-modified composite films were combined with a glucose oxidase-modified alcohol-free sol−gel matrix over the platinum electrode.[15] The catalytic current raised due to the oxidation of the enzymatically produced hydrogen peroxide at 0.65 V was taken as a measure of the glucose concentration.

The performance of the GOx-Zn-XG/CA/PEG biosensor was tested in a thermostated cell within the temperature range 25−45 °C. Its sensitivity increased with the temperature, leveling at a maximum value of 45 °C.

For the development of the hydrogen peroxide biosensor, an HRP layer was applied over the metal-modified film prior to its entrapment into the alcohol-free TEOS, as described above. The enzymatic determination of hydrogen peroxide is based on its bioelectrocatalytic reduction, through the oxidation of ferriperoxidase (Fe^{3+}) to a cation radical (Fe^{4+}) localized on the porphyrin ring or the polypeptide chain and the subsequent mediator-aided reduction of the latter to ferriperodidase.[37] For this reason, our study was performed only on the cathodic region, at −0.2 V. The analytical characteristics of the various biosensors are summarized in Table 5.

The proposed biosensors were also tested in real samples of 1:2000 diluted orange juice and contact lenses cleaner for the determination of glucose and hydrogen peroxide, respectively. The results were compared with those obtained with an enzyme reference F-kit (R-Biopharm GmbH, Germany) for glucose and the potassium permanganate titrimetric method for hydrogen peroxide. The mean relative errors were 2.2 and 1.7%, respectively. The accuracy of the methods was also verified by recovery studies adding 0.1 mM glucose and hydrogen peroxide solutions to samples, respectively. Recoveries were 97−105%.

The working stability of the proposed chemical and biosensors was verified amperometrically by successive injections of 0.1 mM H_2O_2. As a result, the final activity of the composite films (current response versus initial current response × 100) was almost 80% after 100−120 runs. Between measurements the sensors were kept in

(35) Jones, C. W., Ed. *Applications of Hydrogen Peroxide and Derivatives*; RSC: Cambridge, 1999.

(36) Weiss, J. In *Advances in Catalysis and Related Subjects*; Academic Press: New York, 1952; Vol. IV.

(37) Ruzgas, T.; Csöregi, E.; Emeneus, J.; Gorton, L.; Marko-Varga, G. *Anal. Chim. Acta* **1996**, *330*, 123−138.

the buffer solution at room temperature. The sensors displayed good storage stability if stored dry at room temperature when not in use. They retained almost 90−95% of their initial activity after two months of storage at 4 °C. The chemical stability of the xerogels was also investigated. The analytical parameters of two calibration curves, one made one week after the synthesis of the xerogels and one made after fifteen weeks were compared. Observed deviations in dynamic range and the sensitivity of the system were less than 5%.

Acknowledgment. We thank Drs. M. Louloudi and A. Ladavos for the provision of thermogravimetric and SEM/EDS facilities, respectively and EU for funding under the INORGPORE project. Thanks are also extended to Prof. C. E. Efstathiou for fruitful discussions. B.P.S is grateful to the Spanish Ministry of Education and Science for a fellowship supporting her visit to the University of Ioannina.

CM035110U